Effect of higher order couplings in the barrier distribution of $^{12}C+^{142}Nd$ extracted from quasielastic excitation functions

H. Majumdar,* C. Basu, P. Basu, and Subinit Roy
Saha Institute of Nuclear Physics, 1/AF, Bidhannagar, Kolkata 700064, India

K. Mahata, S. Santra, A. Chatterjee, and S. Kailas
Nuclear Physics Division, BARC, Mumbai 400085, India
(Received 11 March 2003; published 24 July 2003)

To explore the effects of higher order coupling on the barrier distribution, we have measured the quasielastic excitation function for $^{12}C+^{142}Nd$ around the nominal Coulomb barrier from 44 to 58 MeV in steps of 1 MeV. Theoretical coupled channel calculations with one and two phonon states were performed using the code ECIS94. The analysis showed that the second order coupling effects explained the barrier distribution profile and excitation function more appropriately than the first order couplings.

DOI: 10.1103/PhysRevC.68.017602 PACS number(s): 25.70.Bc, 24.10.Eq

Single barrier description of fusion reaction evolves into a multiple barrier representation due to coupling of relative motion of two interacting heavy ions with other degrees of freedom, i.e., the inelastic excitations of vibrational or rotational modes and the transfer of particles between the interacting nuclei. The distribution of these effective barriers, as a function of incident energy, carries distinctive signatures of the relevant couplings. However, to construct the barrier distribution from fusion excitation function [1] one needs data of extreme precision ($\sim 1\%$) [2] and furthermore, at above-barrier energies, the distribution is poorly defined as the associated error is inherently large (proportional to fusion cross-section). In recent years an alternative has been proposed [3]. The barrier distribution can also be derived from the complimentary measurement of large angle elastic or quasielastic scattering excitation function, and by definition it involves less error particularly in the higher energy domain. Moreover, it has been conjectured by Kruppa *et al.* [4] that the high energy profile of the barrier distribution might provide information, if any, about the existence of higher order couplings. With the inherent difficulty in obtaining the distribution from higher energy fusion data, the properties of these barriers may be studied better through the large angle elastic and quasielastic scattering measurements.

So far the extraction of barrier distributions from elastic [5–7] and quasielastic [3,6,8–10] scattering data has been reported only for $^{16}O+^{144,152,154}Sm$, $^{16}O+^{186}W$, $^{12}C+^{232}Th$, ^{208}Pb, $^{12,13}C+^{105,106}Pd$, and $^{36}S+^{90,96}Zr$ systems. In none of these studies the effect of higher order and/or multiphonon coupling on the barrier distribution have been investigated. Recently, Takigawa *et al.* [11] explored theoretically the effects of multiphonon excitations on heavy ion fusion near Coulomb barrier energies by using the vibrational limit of the interacting boson model. They showed that the fusion barrier distribution is very sensitive to the anharmonicity of the nuclear surface vibrations. In the case of $^{16}O+^{144}Sm$, they specifically found that the experimental barrier distribution is reproduced only when the correct sign of quadrupole moments of first 2^+ and 3^- states (both negative) are used in the coupled channel calculations. The fusion excitation function, however, is seen to be insensitive to the sign of quadrupole moment of 2^+ state, but it strongly depends on that of the 3^- state.

In this context the present study aims to look at the effects of higher order coupling in describing the large angle *quasielastic excitation function* data and subsequent barrier distribution pattern for ^{12}C scattering from ^{142}Nd nucleus. Like ^{144}Sm ($N=82, Z=62$), ^{142}Nd ($N=82, Z=60$) also has low lying 2^+ and 3^- states as well as double phonon states involving the quadrupole and octupole phonons. We intend to probe the effects of these couplings on the barrier distribution derived from extreme backward angle scattering data for the $^{12}C+^{142}Nd$ system.

The experiment was performed with collimated beam from BARC-TIFR 14UD Pelletron at Mumbai, India. Energy of the projectile was varied from 44 to 58 MeV in steps of 1 MeV. Enriched (98.26%) ^{142}Nd oxide target (thickness $\sim 50\ \mu g/cm^2$) was prepared in a sandwiched form between 5 and 20 $\mu g/cm^2$ carbon backing [12]. Three SSB detector telescopes were used to measure the backangle excitation functions at 150°, 170°, and $-170°$. Twenty-five and 30 μ thick ΔE detectors were used in front of 300 μ stop detectors in the telescope arrangements. Two 300 μ Si(Li) detectors were placed at $\pm 30°$ with respect to the beam direction to monitor Rutherford scattering. The monitors, having apertures of 5 mm, were positioned at a distance of 333 mm from the target. The counts in these detectors were used to normalize the cross-section measurement and to measure angle offset (if any). The defining apertures of three telescopes were, respectively, 3 mm, 2 mm, and 3.2 mm. The energy resolutions of the detectors were found to be less than about 500 keV. As a result the elastic scattering peak was well separated from its neighboring first excited state at all energies. Although the 2_1^+ and 3^- target states could not be clearly resolved, their total yields were measured unambiguously. The $(\Delta E-E)$ detector telescopes performed well and

*Corresponding author. Electronic address: harash@lotus.saha.ernet.in

 ©2003 The American Physical Society

TABLE I. Optical model and deformation parameters (β_n).

System		V_0 (MeV)	r_0 (fm)	a_0 (fm)	W_V (MeV)	r_I (fm)	a_I (fm)	r_C (fm)
^{12}C+^{142}Nd 70.4 MeV	Set *A*	52.0	1.221	0.562	15.0	1.283	0.452	1.25
	Set *B*	20.0	1.315	0.562	11.6	1.341	0.414	1.25
	E^*	J^π	β_λ					Ref.
^{142}Nd	1.576	2^+	0.081					
	2.084	3^-	0.127					[15]
	2.101	4^+	0.0627					
	2.846	2^+	0.0387					
^{12}C	4.430	2^+	−0.460					[13]

reasonably good particle identification for $Z=4$, 5, and 6 was obtained. But owing to high negative Q values for $-1n$, $-2n$, $-1p$, $-2p$, and $-1p1n$ channels the statistics were very low. However, the total quasielastic counts comprising elastic, inelastic, and transfer channels were found to a reasonable accuracy.

In order to explain simultaneously the elastic angular distribution, elastic and quasielastic excitation functions, and the barrier distribution, we have started the analysis with a set of optical model parameters, obtained by fitting the elastic scattering data [13] at $E_{lab}=70.4$ MeV. The potential so obtained is assumed to be reasonably free of coupling effects, as the energy (70.4 MeV) is much above the nominal Coulomb barrier. The fit to the experimental angular distribution with this set of potential parameters (see Table I) is shown in Fig. 1 (solid line). Analysis has also been done with another set of parameters (set *B* in Table I) from Ref. [13]. The elastic angular distribution obtained with these parameters is almost indistinguishable from that obtained with set *A*. The fit with set *B*, therefore, is not shown in Fig. 1. At the elastic excitation function level, the first order calculation with parameters of set *B* describes the higher energy data better than the second order calculation. But both the calculations with set *B* underpredict the data at below barrier region. The underpredictions are still more prominent for the quasielastic excitation function. On the other hand, good overall description is obtained with parameters of set *A*. However, the main reason for the preference of set *A* over set *B*, in light of barrier distributions, will be discussed later. Unless otherwise mentioned, all the subsequent theoretical analyses are done with parameter set *A*. Experimental differential cross sections at $\theta_{lab}=170°$ (relative to the Rutherford scattering, σ_R) for quasielastic (elastic+inelastic+projectile

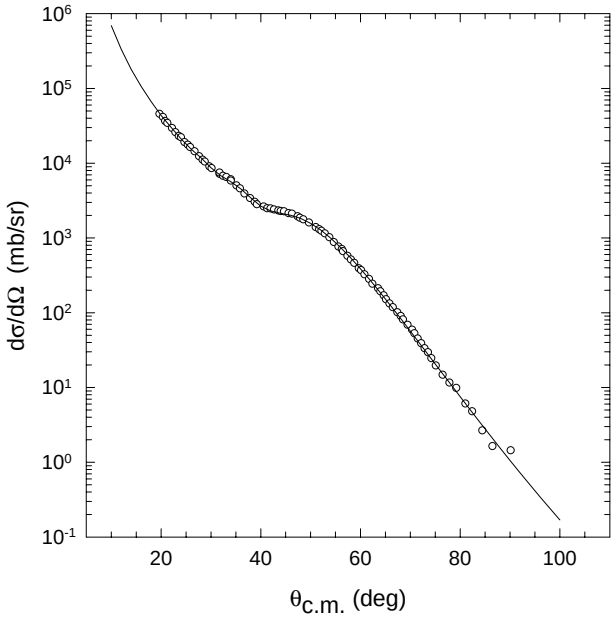

FIG. 1. Optical model fit to the elastic angular distribution data of ^{12}C+^{142}Nd at $E_{lab}=70.4$ MeV [13]. Solid line denotes the fit with the potential parameters from Table I.

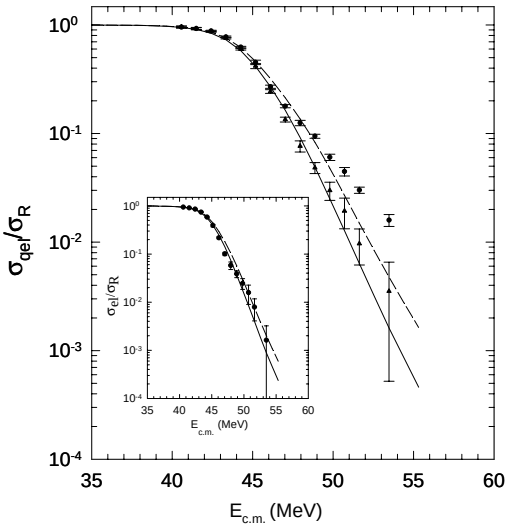

FIG. 2. Coupled channel calculations for excitation functions of ^{12}C+^{142}Nd system. The solid circles and the solid triangles denote the quasielastic and elastic $+2^+ + 3^-$ excitation function data measured at $\theta_{lab}=170°$. The dashed and solid curves are predictions from first and second order CC calculations with ground states, 2^+ and 3^- states with potential set *A*. Inset shows the elastic excitation function data along with corresponding theoretical predictions.

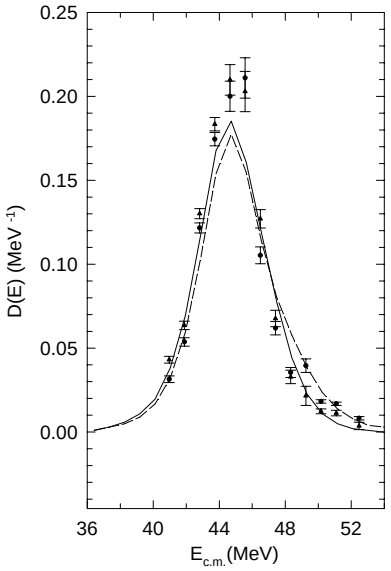

FIG. 3. Barrier distribution functions. Experimental distributions generated from quasielastic (solid circles) and elastic $+2^+ +3^-$ (solid triangles) excitation functions. The theoretical curves correspond to CC calculations as stated in the caption of Fig. 2

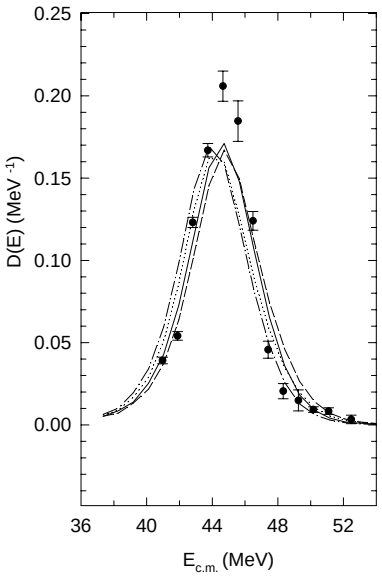

FIG. 4. Barrier distribution functions. Experimental distributions generated from elastic (solid circles) excitation functions. The theoretical curves correspond to CC calculations with potential sets *A* and *B* [13]. Dashed and solid lines correspond to first and second order calculations with set *A*. Dotted and dash-dotted curves refer to the same calculations with set *B*.

excitation+transfer) ($\sigma_{qel}^{exp}/\sigma_R$) (bullet) and for elastic and inelastic (mainly 2^+ and 3^- of the target) scattering ($\sigma_{el+}^{exp}/\sigma_R$) (solid triangle) as functions of energy have been displayed in Fig. 2. Theoretical analysis was done in a coupled channel framework using ECIS94 [14], assuming ^{142}Nd as a vibrator. The scheme included the coupling between the ground state and the excited states 2^+ (1.575 MeV) and 3^- (2.084 MeV) of the target having appreciable coupling strengths. These strengths were taken from experimentally derived coupling amplitudes (β values) [15] and are shown in Table I. Other β values were determined from the scaling relation $\beta_c R_c = \beta_N R_N$. In the analysis, first order coupling includes $0^+ \rightarrow 2^+$ ($L=2$) and $0^+ \rightarrow 3^-$ ($L=3$) and second order quadrupole couplings ($2^+ \otimes 2^+, 3^- \otimes 3^-, 2^+ \otimes 3^-$) were taken into account in addition to the earlier first order ones. These theoretical predictions for σ_{el+}/σ_R are also plotted in Fig. 2 for comparison with the experimental data. It is seen that ECIS first order calculation overestimates the experimental excitation function σ_{el+}/σ_R. But the second order prediction yields a reasonable fit to the experimental data. It is to be noted that the experimantal $\sigma_{qel}^{exp}/\sigma_R$ and $\sigma_{el+}^{exp}/\sigma_R$ exhibit a small change of slope around $E_{\text{c.m.}} \sim 46.5$ MeV. But such deviation is not visible in the theoretical curves. We also tried coupling to other target states in addition to 2^+ and 3^-, but they did not produce appreciably different results than those already obtained. At the above barrier energies only a fraction of scattered flux is carried by the elastic and the two inelastic channels that have been taken into account explicitly in the coupled channel calculations. Experimental quasielastic excitation functions show that at higher energies scattering flux may include significant contribution from projectile excitation (2^+ of ^{12}C) and other probable transfer channels. Even after the subtraction of the contribution from projectile excitation, the excitation function $\sigma_{el+}^{exp}/\sigma_R$ (solid triangles) still carries the indication of contributions from other reaction channels than the elastic, 2_1^+ and 3_1^- channels considered explicitly. Contributions from transfer channels may be the possible cause for the deviation. However, the trends of the calculated excitation functions clearly show that the curve that includes the second order couplings describes the overall excitation function data quite well and with possible subtraction of transfer contribution the fit can further improve.

In the adiabatic and isocentrifugal approximation, the quasielastic differential cross section in the presence of multiple barriers may be represented as a weighted sum of eigen channel elastic differential cross sections ($d\sigma_\alpha$). Hence the barrier distribution [D_{qel}(E)] can be extracted from the quasielastic excitation function as follows:

$$D_{qel}(E) = -\frac{d}{dE}\left(\frac{d\sigma_{qel}}{d\sigma_R}\right) = \sum_\alpha w_\alpha \frac{d}{dE}\left(\frac{d\sigma_\alpha}{d\sigma_R}\right), \qquad (1)$$

where w_α, $d\sigma_{qel}$, and $d\sigma_R$ are, respectively the α channels barrier weight, quasielastic scattering differential cross section, and Rutherford scattering differential cross section. It is clear that D_{qel} reflects the distribution of barrier weights. The above formulation requires excitation functions at 180°, but experimentally it is difficult to measure at this backward most angle. We extracted experimental D_{qel} at 170° from Eq. (1) by employing a point difference method. To compare it with the barrier distribution at 180°, the energy scale was reduced by the centrifugal energy E_{cent} given by

$$E_{cent} = E_{\text{c.m.}} \frac{\csc(\theta_{\text{c.m.}}/2 - 1)}{\csc(\theta_{\text{c.m.}}/2 + 1)}, \qquad (2)$$

where $\theta_{\mathrm{c.m.}}$ and $E_{\mathrm{c.m.}}$ represent, respectively, the detection angle and the projectile energy in the center-of-mass system. The barrier distributions $D_{qel}(E)$ have been extracted at the energy interval of 1 MeV. Similarly, a barrier distribution $D_{el+}^{exp}[=-d(\sigma_{el+}^{exp}/\sigma_R)/dE]$ was found out from the experimental σ_{el+}^{exp} values. Figure 3 represents these distributions together with the theoretical predictions at 180° from single phonon and double phonon coupled channel calculations with ECIS94.

The distinction between the first order and the second order calculations is again clearly visible in the fits to the barrier distribution data (Fig. 3). Second order prediction of barrier distribution presents much better fit to the data (D_{el+}^{exp}) both in the lower and higher energy domains than the first order calculation. It is to be noted that the distribution $D_{qel}^{exp}(E)$ carries the indication of some peaklike structures in the higher energy side beyond 48 MeV that almost disappears from $D_{el+}^{exp}(E)$. The theoretical distribution functions calculated with 2^+ and 3^- couplings do not show any such structures at the higher energy side and the curve (solid line) calculated with second order couplings provides an excellent fit to the smooth fall of the distribution $D_{el+}^{exp}(E)$. With the structures in the higher energy side appearing due to transfer coupling and coupling to projectile excitation, a full CRC calculation is in progress including these couplings in the scheme to reproduce the distribution $D_{qel}^{exp}(E)$.

Finally to justify our preference for optical model parameters set *A* over set *B* [13], we have compared in Fig. 4 the barrier distribution generated from the elastic scattering data only with the theoretical distributions obtained from parameter sets *A* and *B*. The distributions resulted from first and second order calculations with set *B* show clear shifts towards lower energy side. The second order calculation with potential parameter set *A* not only reproduced the peak position nicely, but also generated reasonably well the fall of the distribution on higher and lower energy sides. It would be an interesting study to look for the effect of choice of potential parameters on barrier distribution.

In summary, we have measured the quasielastic excitation functions for $^{12}C+^{142}Nd$ around the nominal Coulomb barrier at three backward angles in 1 MeV energy steps. Barrier distribution functions were generated for the first time from quasielastic excitation functions using a simple point difference formula. Theoretical coupled channel calculations with one and two phonon states were performed using the code ECIS94. Theoretical analysis with ECIS94 showed that the second order coupling effects explain more appropriately the structure of the barrier distributions and the excitation functions than the first order couplings. Though these estimates show reasonable agreement with the experimental observations, the effects of transfer couplings and anharmonicity need to be explored for a full understanding.

[1] N. Rowley, G.R. Satchler, and P.H. Stelson, Phys. Lett. B **254**, 25 (1991).

[2] J.X. Wei, J.R. Leigh, D.J. Hinde, J.O. Newton, R.C. Lemmon, S. Elfstrom, J.X. Chen, and N. Rowley, Phys. Rev. Lett. **67**, 3368 (1991).

[3] H. Timmers, J.R. Leigh, M. Dasgupta, D.J. Hinde, R.C. Lemmon, J.C. Mein, C.R. Morton, J.O. Newton, and N. Rowley, Nucl. Phys. **A584**, 190 (1995).

[4] A.T. Kruppa, P. Roman, M.A. Nagarajan, and N. Rowley, Nucl. Phys. **A560**, 845 (1993).

[5] N. Rowley, H. Timmers, J.R. Leigh, M. Dasgupta, D.J. Hinde, R.C. Lemmon, J.C. Morton, C.R. Morton, and J.O. Newton, Phys. Lett. B **373**, 23 (1996).

[6] Huanguiao Zhang, Feng Yang, Chengjian Lin, Zuhua Liu, and Yueming Hu, Phys. Rev. C **57**, R1047 (1998).

[7] A.M. Stefanini, L. Corradi, A.M. Vinodkumar, Yang Feng, F. Scarlassara, G. Montagnoli, S. Beghini, and M. Bisogna, Phys. Rev. C **62**, 014601 (2000).

[8] Shrabani Sinha, M.R. Pahlavani, R. Varma, R.K. Choudhury, B.K. Nayak, and A. Saxena, Phys. Rev. C **64**, 024607 (2001).

[9] O.A. Capuro, J.E. Testoni, D. Abriola, D.E. DiGregorio, G.V. Marti, A.J. Pacheco, M.R. Spinella, and E. Achterberg, Phys. Rev. C **62**, 014613 (2000).

[10] S. Santra, P. Singh, S. Kailas, A. Chatterjee, A. Shrivastava, and K. Mahata, Phys. Rev. C **64**, 024602 (2000).

[11] N. Takigawa, K. Hagino, and S. Kuyucak, J. Phys. G **23**, 1367 (1997).

[12] Samit Mandal, D. Kabiraj, and D.K. Avasthi, Nucl. Instrum. Methods Phys. Res. A **397**, 59 (1997).

[13] D.L. Hillis, E.E. Gross, D.C. Hensley, C.R. Bingham, F.T. Baker, and A. Scott, Phys. Rev. C **16**, 1467 (1977).

[14] J. Raynal, ECIS94 (unpublished).

[15] M. Pignanelli, N. Blasi, J.A. Bordewijk, R. DeLeo, M.N. Harakeh, M.A. Hofstee, S. Micheletti, R. Perrino, V. Yu Ponomarev, V.J. Soloviev, A.V. Sushkov, and S.Y. van der Werf, Nucl. Phys. **A559**, 1 (1993); R.K.J. Sandor, H.P. Blok, U. Garg, M.N. Harakeh, C.W. de Jaeger, V. Yu Ponomarev, A.I. Vdovin, and H. de Vries, *ibid.* **A535**, 669 (1991).